Main-Group Elements

DOI: 10.1002/anie.201207529

2,2-Bipyridine Complexes of Antimony: Sequential Fluoride Ion Abstraction from SbF_3 by Exploiting the Fluoride Ion Affinity of Me_3Si^+**

Saurabh S. Chitnis, Neil Burford, and Michael J. Ferguson*

The coordination chemistry of the p-block elements as Lewis acceptors is superficially developed relative to that of the transition metals, despite the ability of the heavy p-block elements to access coordination numbers of six or greater. Consequently, many compounds of the heavy elements adopt coordination polymeric arrays in the solid state through intermolecular donor–acceptor interactions. Molecular complexes are known for many p-block element acceptors which are analogous to transition-metal complexes, with a neutral ligand (L) providing an additional bond to a neutral acceptor center (E; p-block element), even with retention of a lone pair at the acceptor site [Eq. (1)]. Alternatively, a neutral ligand can displace an anionic substituent (X; leaving group) to introduce a cationic charge on the complex, depending on the relative bond strengths of E–X and E–L, and the lattice energy of the resulting salt [Eq. (2)]. Such coordinative interactions are more generally applicable when the E–X bond is activated by an abstracting agent (A) [Eq. (3)]. The activation of a second E–X bond [Eq. (4)] increases the Lewis acidity of the acceptor, thus enabling a diversification of coordination chemistry, but examples are rare,[1,2] as are examples of heterolytic cleavage of a third E–X bond [Eq. (5)].[3–5]

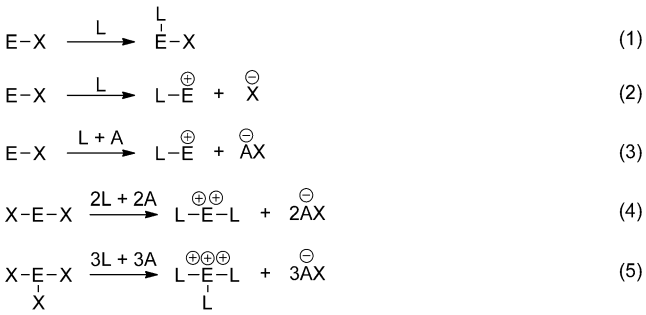

In an attempt to systematically and rationally augment the Lewis acidity of p-block elements and develop the coordination chemistry of p-block elements, we have examined a variety of reagent combinations of an element halide with a halide abstracting agent and a neutral ligand, and have discovered that mixtures of SbF_3, $Me_3SiOSO_2CF_3$ (TMSOTf), and 2,2-bipyridine (bipy) in acetonitrile give compounds **1**, **2**, and **3** in high yield upon isolation depending on the applied stoichiometry (*n* and *m*; see Scheme 1). The substantial thermodynamic preference for the formation of Me_3SiF (b.p. 16.5 °C) is evidenced by gaseous evolution and by the characteristic doublet in the ^{1}H NMR spectrum of the reaction mixture.

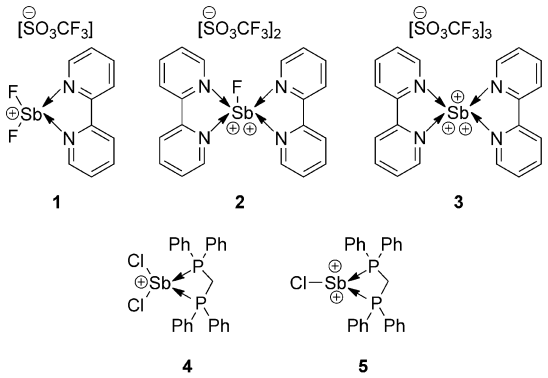

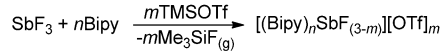

Scheme 1. Synthesis of compounds **1** ($n=m=1$), **2** ($n=m=2$), and **3** ($n=2$, $m=3$) by the stoichiometric abstraction of fluoride ions from SbF_3 by $[Me_3Si]^+$.

Compounds **1**, **2**, and **3** were isolated and characterized using NMR spectroscopy and elemental analysis. All are extremely moisture sensitive and exposure of the solid results in protonation of the ligands within minutes. The X-ray structures of **1** and **3** are shown in Figures 1 a and b, respectively, and selected structural parameters are listed in Table 1. It has not yet been possible to determine the solid-state structure of compound **2**. The solid-state structure of **1** is best described as a triflate salt of a difluorostibenium cation, $[SbF_2]^+$, which is asymmetrically chelated at antimony by a bipy ligand. The antimony center also engages in weak interactions with one oxygen atom of the anion and a fluorine

[*] S. S. Chitnis, Prof. N. Burford
Department of Chemistry, University of Victoria
P.O Box 3065, Stn. CSC, Victoria, BC (Canada)
E-mail: nburford@uvic.ca
Dr. M. J. Ferguson
X-ray Crystallography Laboratory
Department of Chemistry, University of Alberta
11227 Saskatchewan Drive NW, Edmonton, AB (Canada)

[**] We thank the Natural Sciences and Engineering Council of Canada, the Canada Foundation for Innovation, and the Vanier Canada Graduate Scholarships Program for funding.

Supporting information for this article (spectroscopic details) is available on the WWW under http://dx.doi.org/10.1002/anie.201207529.

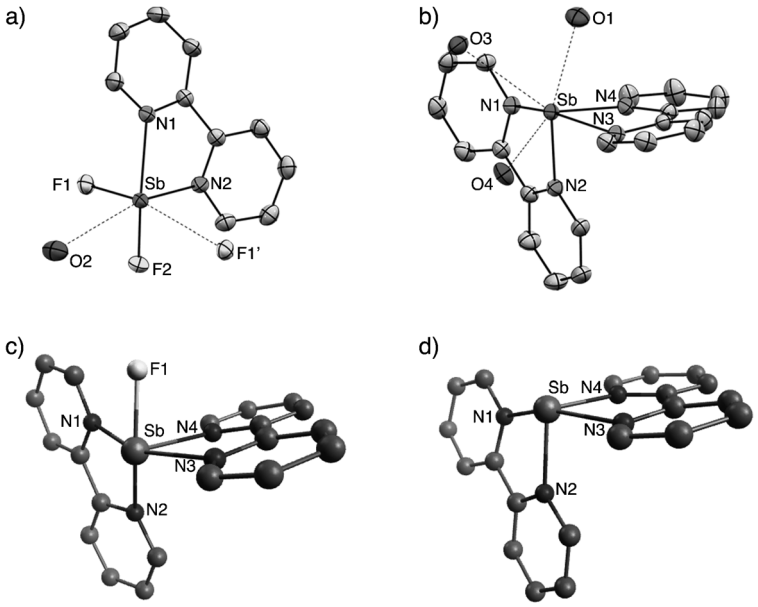

Figure 1. Views of the antimony environment in the solid-state structures of a) **1**, and b) **3**, showing selected (interacting) oxygen atoms of the triflate anions. Thermal ellipsoids are drawn at the 50% probability level. Calculated gas-phase structures of the cations in **2** (c) and **3** (d). Hydrogen atoms are omitted for clarity.[15]

atom of a neighboring $[SbF_2]^+$ unit, thus imposing an overall distorted octahedral geometry at antimony.

The solid-state structure of **3** is best described as a tris-(triflate) salt of an $[Sb]^{3+}$ cation chelated by two bidentate bipy ligands. The antimony center shows weak contacts with three oxygen atoms of the triflate anions. The ^{19}F NMR spectra of **1** and **2** show signals for the $[SbF_2]^+$ and $[SbF]^{2+}$ fragments at $\delta = -90.1$ ppm and $\delta = -93.3$ ppm, respectively, and they are severely broadened by the quadrupolar spins of the antimony nuclides [$I(^{121}Sb) = 5/2$, $I(^{123}Sb) = 7/2$]. The ^{19}F NMR signals corresponding to the triflate anions in **1**, **2**, and **3** are characteristically sharp at $\delta = -79.5$ ppm, and indicative of dissociated $[SO_3CF_3]^-$ ions in solution. The optimized DFT (B3LYP/Def2-TZVPP) structure for the cation of **3** in the gas phase is consistent with the observed solid-state structure showing the AB_4E VSEPR geometry for Sb and implicating a stereochemically active lone pair. The hypothetical C_{2v} (square-based pyramid), D_{2h} (square-planar N_4), and S_4 (tetrahedral N_4) structures for $[(bipy)_2Sb]^{3+}$ are not global minima and are all higher in energy than the AB_4E structure.

Table 1: Selected bond lengths [Å] and angles [°] within the cations in compounds **1**, **2**, and **3**.[a]

	1	2	3
Sb–N1	2.3719(18) [2.429]	[2.342]	2.2843(12) [2.286]
Sb–N2	2.2302(18) [2.258]	[2.502]	2.2333(12) [2.192]
Sb–N3		[2.384]	2.3322(12) [2.286]
Sb–N4		[2.254]	2.2434(12) [2.192]
Sb–O1			2.5978(12)
Sb–O2	2.9416(19)		2.6499(12)
Sb–O3			3.077(1)
Sb–F1	1.9332(13) [1.900]	[1.942]	
Sb–F2	1.9387(13) [1.938]		
Sb–F1′	2.7566(13)		
N1-Sb-N2	69.70(6) [69.4]	[67.6]	72.09(4) [73.6]
N1-Sb-N3		[159.1]	156.02(4) [157.9]
N1-Sb-N4		[91.7]	87.87(4) [91.4]
N2-Sb-N3		[117.6]	91.42(4) [91.4]
N2-Sb-N4		[80.2]	78.66(4) [95.5]
N3-Sb-N4		[70.4]	71.53(4) [73.6]
N1-Sb-F2	143.26(6) [150.0]		
N2-Sb-F1	95.78(6) [94.8]	[145.2]	
N2-Sb-F2	83.13(6) [83.2]		
F1-Sb-F2	83.92(6) [73.6]		

[a] Square brackets denote values calculated for the cations in the gas phase at the B3LYP/Def2-TZVPP level.

The Sb–N bond distances in **1** and **3** are slightly longer (0.13–0.23 Å) than the sum of the covalent radii (Sb–N = 2.10 Å), while the Sb–O (triflate) distances are substantially longer (0.55–1.02 Å) than the sum of the covalent radii (Sb-O = 2.05 Å), thus implicating a degree of ionicity, as illustrated by the structures of **1** and **3**. The Sb–F bond lengths in **1** [1.9332(13) Å and 1.9387(13) Å] are substantially shorter than the inter-ion Sb–F contact [2.7566(13) Å] between adjacent $[SbF_2]^+$ units. Within the respective sums of the van der Waals' radii (Sb–N = 3.55 Å; Sb–O = 3.52 Å; Sb–F = 3.47 Å), the antimony centers adopt a six (**1**) or seven (**3**) coordinate geometry, as illustrated in Figure 1. While the distortions from ideal octahedral or pentagonal bipyramidal geometry are due to the influence of a stereochemically active lone pair and the steric strain of the rigid bipy ligand, there may also be contributions resulting from the packing of the ions. In **3**, O1, O3, and O4 lie 37° below, 38° above, and 32° above, respectively, the plane defined by N4, Sb, and N2. The average Sb–N distance [2.317(4) Å][6] in the neutral complex $(bipy)SbF_3$ is slightly longer than that in **1** [2.3011(36) Å] and substantially longer than that in **3** [2.2733(48) Å], despite the steric restrictions imposed by the presence of a second bipy ligand in **3**. The trend in Sb-N distances correlates with an increase in the charge at the Sb center going from $(bipy)SbF_3$ to **3**. The C–C bond length between the pyridine rings of the bipy ligand in both cations [1.476(4) Å in **1**; 1.474(2) and 1.477(2) Å in **3**] is consistent with a single C–C bond (1.50 Å in free bipy),[14] thus discounting oxidation of bipy on interaction with the antimony cation.

The $[SbF_2]^+$ moiety in **1** can be compared with the only structurally characterized examples of difluoropnictenium ions in $[AsF_2][SbF_6]$[7] and $[K/NH_4][SbF_2][HAsO_4]$.[8] The Sb–F bond lengths [1.9332(13) Å and 1.9387(13) Å] in **1** are significantly shorter than the sum of the covalent radii for Sb and F ($\Sigma_{r,cov} = 2.03$ Å), and are slightly shorter than the Sb–F bonds in $[K/NH_4][SbF_2][HAsO_4]$ [1.959(2) Å and 1.995(2) Å for K; 1.953(4) Å and 1.999(4) Å for NH_4]. Consistent with

the trends observed in the Sb–N distances, the Sb–F bonds in **1** are approximately 0.1 Å shorter than those in neutral (bipy)SbF_3 and are comparable to those observed in compounds featuring $[SbF]^{2+}$ centers with strongly interacting anions {1.934(4) Å in [Na][SbF][PO_4]; 1.923(4) Å in [NH_4]-[SbF][PO_4]}.[9]

Table 1 lists the results from DFT (B3LYP/Def2-TZVPP) geometry optimizations of cations in **1**, **2**, and **3** in the gas phase. The calculated Sb–N bonds in $[(bipy)SbF_2]^+$ and $[(bipy)_2Sb]^{3+}$ are on average 0.069 Å longer and 0.034 Å shorter, respectively, than those observed in the solid-state structures. There is no significant variation between the observed and calculated bond angles for $[(bipy)SbF_2]^+$. In contrast, comparison of the bond angles for $[(bipy)_2Sb]^{3+}$ clearly show that the presence of three anion contacts in the plane of N2 and N4 in the solid-state structure of **3** causes a compression of the angle between the two bipy ligands [calcd.: 95.55°, expt.: 78.66(4)°].

The calculated Sb–F bond length in $[(bipy)_2SbF]^{2+}$ is essentially the same as the observed and calculated Sb–F bonds in **1**, thus suggesting that the increased charge in the dication is effectively offset by the presence of a second bipy ligand. Consistently, the calculated Sb–N bond lengths in $[(bipy)_2SbF]^{2+}$ are on average 0.130 Å longer than those calculated for $[(bipy)_2Sb]^{3+}$, thus indicating accommodation of molecular charge in the Sb–N bonds. The alternate VSEPR C_{2v} square-based pyramid (AB_4CE) geometry for $[(bipy)_2SbF]^{2+}$ was calculated to be 22 kJ mol^{-1} higher than the minimum energy structure in Figure 1c.

NBO analysis for $[(bipy)_2Sb]^{3+}$ gives a residual charge of $+1.77e$ at the Sb atom, thus indicating a substantial Lewis acidity. Furthermore, the LUMO of $[(bipy)_2Sb]^{3+}$ (Figure 2)

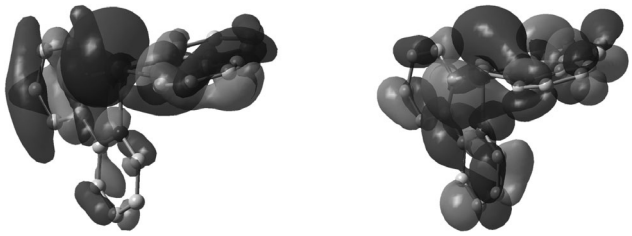

Figure 2. Surface plots (isovalue = 0.02) showing the HOMO−2 (left) and LUMO (right) in the gas-phase structure of $[(bipy)_2Sb]^{3+}$. Hydrogen atoms omitted for clarity.

shows two large lobes at Sb *trans* to the N2-Sb and N4-Sb bonds, thereby inviting interaction from a third chelate. The optimized structure for $[(bipy)_3Sb]^{3+}$ in the gas phase is approximately 250 kJ mol^{-1} lower in energy than that of $[(bipy)_2Sb]^{3+}$ and dissociated bipy. Nevertheless, attempts to form $[(bipy)_3Sb]^{3+}$ from reactions of **3** with excess bipy or from reaction mixtures of SbF_3 with excess bipy and excess TMSOTf have not been successful. We conclude that the tris(bipy) complexes which are commonplace in transition-metal chemistry are precluded for antimony because of the presence of a stereochemically active 5s lone pair (HOMO−2) in $[(bipy)_2Sb]^{3+}$, and thus imposes a significant kinetic barrier to association of the third ligand molecule.

Consideration of the bond angles in **1** and **3** provides qualitative insight into the acceptor orbitals at the antimony center. In compound **1**, the F1-Sb-N2 and F2-Sb-N2 angles [95.78(6)° and 83.13(6)°, respectively] indicate that N2 interacts with the vacant p orbital which is orthogonal to the F-Sb-F plane. The slightly longer Sb–N1 interaction is presumably due to the *trans* influence of the Sb–F2 bond. In compound **3**, where four N donors are present, two sets of three approximately orthogonal N–Sb interactions (corresponding to three vacant p-orbitals of Sb^{3+}) are evident, with deviation from the idealized 90° angle because of restrictions imposed by the chelate interaction and possibly the presence of a stereochemically active 5s lone pair. Thus, the average N-Sb-N angle involving Sb–N1, Sb–N4, and Sb–N2 bonds is 79.54° and the average N-Sb-N angle involving Sb–N2, Sb–N3, and Sb–N4 bonds is 80.57°. For comparison, the gas-phase[10] and solid-state[11] structures of SbF_3 show F-Sb-F angles of 94.8(2)° and 87.3(3)°, respectively.

The chelate bipy complexation of $[SbF_2]^+$ is analogous to that observed for the interaction of bis(diphenylphosphino)-methane (dppm) with $[SbCl_2]^+$ in cation **4**,[2] thus illustrating retention of a pyramidal geometry at antimony and asymmetric chelation. In contrast to compound **2**, in which $[SbF]^{2+}$ accommodates two bipy ligands, $[SbCl]^{2+}$ engages only one dppm in complex **5**.[2] Mixtures of **5** with excess dppm and excess halide abstracting agent show no evidence of formation of a $[(dppm)_nSb]^{3+}$ complex. Similarly, mixtures of $SbCl_3$, TMSOTf, and bipy initially show formation of the chloride derivatives (bipy)$SbCl_2$(OTf) and $(bipy)_2SbCl(OTf)_2$, and **3** is only observed in a trace amount when the reaction mixtures are subjected to removal (under vacuum) of Me_3SiCl followed by addition of excess TMSOTf.

To understand the thermodynamic factors that enable fluoride ion abstraction from $[SbF]^{2+}$ and preclude the chloride ion abstraction from $[SbCl]^{2+}$, we have computed the reaction enthalpy for halide transfer from antimony to silicon according to Equation (8) (Table 2). To assess their relative thermodynamic contributions, the E–X heterolytic bond strengths [for half-reactions see Eqs. (6) and (7)] were also estimated by using an isodesmic scheme which incorporates experimentally known halide ion affinities for $AlCl_3$ as reference reactions. The enthalpies for the reactions in Equations (6)–(8) show that halide transfer from antimony

$$SbX_3 \longrightarrow [Sb]^{3+} + 3[X]^- \quad (6)$$

$$3[Me_3Si]^+ + 3[X]^- \longrightarrow 3Me_3SiX \quad (7)$$

$$SbX_3 + 3[Me_3Si]^+ \longrightarrow [Sb]^{3+} + 3Me_3SiX \quad (8)$$

to silicon is substantially more favorable for SbF_3 than for $SbCl_3$, because the heterolytic association of three Si–F bonds is 607 kJ mol^{-1} more exothermic than the heterolytic association of three Si–Cl bonds, whereas the heterolytic cleavage of three fluoride ions from SbF_3 is only 463 kJ mol^{-1} more endothermic than the heterolytic cleavage of three chloride ions from $SbCl_3$. Consequently, the fluoride ion affinity of the hypothetical $[Me_3Si]^+$ cation (950 kJ mol^{-1}; cf. 965 kJ mol^{-1} at

the MP2 level[12]) renders Equation (8) more favorable for X = F, and is consistent with the experimental observations.

Table 2: Calculated (B3LYP/Def2-TZVPP) reaction enthalpies (kJ mol^{-1}).

Reaction	ΔH_{rxn}(X=F)	ΔH_{rxn}(X=Cl)	ΔH_{rxn}(F) − ΔH_{rxn}(Cl)
(6)[a]	5275	4812	463
(7)[a]	−2850	−2243	−607
(8)	2425	2569	−144

[a] Reaction enthalpies calculated from isodesmic reactions using experimentally known halide ion affinities of $AlCl_3$ and calculated halide ion affinities of $[SbX_n]^{(3-n)+}$ and $[Me_3Si]^+$ (see the Supporting Information). The values correspond to the complete dissociation of $[X]^-$ ions from SbX_3 [Eq. (6)], the association of $[X]^-$ ions with $[Me_3Si]^+$ [Eq. (7)], and the halide transfer from SbX_3 to $3[Me_3Si]^+$ [Eq. (8)].

In conclusion, by exploiting the thermodynamically favorable elimination of gaseous Me_3SiF from the rapid reaction of SbF_3 with a highly fluoro-acidic silyl reagent,[13] we have discovered a high-yield approach to sequential fluoride ion abstraction to give a series of bipy complexes containing $[SbF_2]^+$, $[SbF]^{2+}$, and $[Sb]^{3+}$ acceptors. The formation of a fluorosilane provides a potentially general approach to enhance the Lewis acidity and coordination chemistry of p-block centers.

Experimental Section

1·CH_3CN: SbF_3 (0.179 g, 1 mmol) and bipy (0.156 g, 1 mmol) were stirred in CH_3CN (10 mL) for 0.25 h at 23 °C. A solution of TMSOTf (0.222 g, 1 mmol) in CH_3CN (5 mL) was added. After stirring for 4 h, the reaction mixture was filtered and concentrated to 5 mL. A crystalline material formed at −30 °C. Yield: 0.275 g (0.59 mmol, 59 %, crystals); m.p. 173–177 °C. C,H,N analysis (%): calcd: C 28.41, H 1.73, N 6.02; found: C 28.00, H 1.86, N 5.97. Crystal data: CCDC 901271, $C_{11}H_8F_5N_2O_3SSb$, size $0.64 \times 0.36 \times 0.35$ mm^3, monoclinic, $P2_1/c$, $a = 9.1312(4)$, $b = 18.5598(9)$, $c = 8.9512(4)$ Å, $\beta = 110.1717(4)°$, $V = 1423.94(11)$ Å^3, $Z = 4$, $\mu = 2.157$ mm^{-1}, $2\theta_{max} = 52.82$, collected (independent) reflections = 11 220 (2920), 208 parameters, $R1 = 0.0195$, $wR2 = 0.0485$ for all data, max/min residual electron density = 0.770/−0.454 e Å^{-3}.

2: SbF_3 (0.179 g, 1 mmol) and bipy (0.312 g, 2 mmol) were stirred in CH_3CN (10 mL) for 0.25 h. A solution of TMSOTf (0.444 g, 2 mmol) in CH_3CN (5 mL) was added. After stirring for 16 h at 23 °C, the volatiles were removed in vacuum and the solid was recrystallized from CH_3CN and washed with cold CH_3CN and Et_2O to obtain a fine white powder. Yield: 0.635 g (0.84 mmol, 84 %, washed powder); m.p. 170–173 °C. C,H,N analysis (%): calcd: C 35.17, H 2.15, N 7.46; found: C 35.02, H 2.16, N 7.50.

3·CH_3CN: TMSOTf (8.000 g, 36 mmol) in CH_3CN (20 mL) was cautiously added (exothermic) in two portions, 10 h apart, to a mixture of SbF_3 (1.785 g, 10 mmol) and bipy (3.130 g, 20 mmol) at 23 °C. After stirring for an additional 4 h at 23 °C, the volatiles were removed in vacuum and the solid was recrystallized from CH_3CN at −30 °C. Yield: 7.611 g (8.3 mmol, 83 %, crystals); Coordinated CH_3CN was removed under vacuum: m.p. 111–114 °C. C,H analysis (%): calcd: C 31.34, H 1.83; found: C 31.55, H 1.72. Crystal data: CCDC 901270, $C_{25}H_{19}F_9N_5O_9S_3Sb$, size $0.43 \times 0.32 \times 0.15$, triclinic, $P\text{-}1$, $a = 9.0855(3)$, $b = 13.2629$ (4), $c = 13.8870(4)$, $\alpha = 81.6469(3)°$, $\beta = 86.8308(3)$, $\gamma = 84.9286(3)°$, $V = 1647.62(9)$ Å^3, $Z = 2$, $\mu = 1.137$ mm^{-1}, $2\theta_{max} = 55.06$, collected (independent) reflections = 14 727 (7519), 470 parameters, $R1 = 0.0187$, $wR2 = 0.0501$ for all data, max/min residual electron density = 0.424/−0.431 e Å^{-3}.

Received: September 17, 2012
Revised: November 24, 2012
Published online: January 7, 2013

Keywords: antimony · coordination modes · fluoride · N ligands · structure elucidation

[1] J. L. Dutton, P. J. Ragogna, *Coord. Chem. Rev.* **2011**, *255*, 1414 – 1425.
[2] a) S. S. Chitnis, B. Peters, E. Conrad, N. Burford, R. McDonald, M. J. Ferguson, *Chem. Commun.* **2011**, *47*, 12331 – 12333; b) A. L. Brazeau, A. S. Nikouline, P. J. Ragogna, *Chem. Commun.* **2011**, *47*, 4817 – 4819.
[3] C. W. Makosky, G. E. Galloway, G. E. Ryschkewitsch, *Inorg. Chem.* **1967**, *6*, 1972 – 1974.
[4] I. Vargas-Baca, M. Findlater, A. Powell, K. V. Vasudevan, A. H. Cowley, *J. Chem. Soc. Dalton Trans.* **2008**, 6421 – 6426.
[5] a) J. J. Weigand, K. O. Feldmann, A. K. C. Echterhoff, A. Ehlers, K. Lammertsma, *Angew. Chem.* **2010**, *122*, 6314 – 6317; *Angew. Chem. Int. Ed.* **2010**, *49*, 6178 – 6181; b) J. Petuškova, M. Patil, S. Holle, C. W. Lehmann, W. Thiel, M. Alcarazzo, *J. Am. Chem. Soc.* **2011**, *133*, 20758 – 20760; c) R. Garbe, B. Vollmer, B. Neumüller, J. Pebler, K. Dehnicke, *Z. Anorg. Allg. Chem.* **1993**, *619*, 271 – 276.
[6] S. L. Benjamin, J. Burt, W. Levason, G. Reid, M. Webster, *J. Fluorine Chem.* **2012**, *135*, 108 – 113.
[7] A. J. Edwards, R. J. C. Sillis, *J. Chem. Soc. A* **1971**, 942 – 945.
[8] K. Holz, R. Mattes, *Z. Anorg. Allg. Chem.* **1989**, *578*, 133 – 142.
[9] R. Mattes, K. Holz, *Angew. Chem.* **1983**, *95*, 898; *Angew. Chem. Int. Ed. Engl.* **1983**, *22*, 872.
[10] J. Molnár, M. Kolonits, M. Hargittai, *J. Mol. Struct.* **1997**, *413 – 414*, 441 – 446.
[11] A. J. Edwards, *J. Chem. Soc. A* **1970**, 2751 – 2753.
[12] J. M. Slattery, S. Hussein, *Dalton Trans.* **2012**, *41*, 1808 – 1815.
[13] R. Haiges, A. Vij, J. A. Boatz, S. Schneider, T. Schroer, M. Gerken, K. O. Christe, *Chem. Eur. J.* **2004**, *10*, 508 – 517.
[14] L. L. Merritt, E. Schroeder, *Acta Crystallogr.* **1956**, *9*, 801 – 804.
[15] CCDC 901271 (**1**) and CCDC 901270 (**3**) contain the supplementary crystallographic data for this paper. These data can be obtained free of charge from The Cambridge Crystallographic Data Centre via www.ccdc.cam.ac.uk/data_request/cif.

